

1985

**N 86 - 24510**

NASA/ASEE SUMMER FACULTY RESEARCH FELLOWSHIP PROGRAM

MARSHALL SPACE FLIGHT CENTER

THE UNIVERSITY OF ALABAMA AT HUNTSVILLE

THE EFFECT OF GROWTH RATE ON THE  
COMPOSITIONAL VARIATIONS IN DIRECTIONALLY

SOLIDIFIED  $\text{Hg}_{1-x}\text{Cd}_x\text{Se}$  ALLOYS

Prepared By:	Rosalia N. Andrews, Ph.D.
Academic Rank:	Associate Professor
University and Department:	Department of Materials Engineering University of Alabama at Birmingham
NASA/MSFC:	
Division:	Low Gravity Science
Branch:	Solid State and Solidification Physics
MSFC Counterpart:	Sandor L. Lehoczky Frank R. Szofran
Date:	August 14, 1985
Contract No.:	NGT-01-008-021 The University of Alabama at Huntsville

THE EFFECT OF GROWTH RATE ON THE  
COMPOSITIONAL VARIATIONS IN DIRECTIONALLY  
SOLIDIFIED  $\text{Hg}_{1-x}\text{Cd}_x\text{Se}$  ALLOYS

BY

Rosalia N. Andrews  
Associate Professor of Materials Engineering  
University of Alabama at Birmingham  
Birmingham, Alabama 35294

ABSTRACT

Several  $\text{Hg}_{1-x}\text{Cd}_x\text{Se}$  crystals of composition  $x = 0.2$  were grown in a Bridgman-type directional solidification furnace at varying translation rates. The influence of growth rate on both the longitudinal and radial compositional uniformity for the crystals was determined using density measurements and infrared transmission-edge mapping.

## ACKNOWLEDGEMENTS

I would like to express my appreciation to Gerald Karr, Leroy Osborn, Jim Dozier, and Larry Freeman for putting together a summer program which was very informative and enjoyable. I would also like to acknowledge the financial support of the Space Science Lab for my position on the ASEE/NASA Summer Faculty Fellowship Program.

Thanks go to Alice Dorries for performing the precision density measurements and to Ron Harris for his expert assistance in the slicing of crystals and in metallographic sample preparation. Thanks are also extended to Shirley Buford for her friendship and secretarial support this summer, and to Tony Xudis and Ching Hua Su, my labmates, for their assistance in various aspects of the laboratory work. Special thanks go to Frank Szofran for his day to day help and guidance in the conduction of the laboratory experiments. Also, his ability to work with and modify the IR transmission analysis system used in this project was invaluable to the successful conduction of the work.

Most of all I would like to express my sincere appreciation to both my NASA counterparts, Alex Lehoczky and Frank Szofran. Their interest in the project and involvement on a daily basis made my ten weeks a most enjoyable and professionally rewarding experience. Their patience in explaining the theory and guiding me through the many various operations in the laboratory was critical to my developing a working understanding of the project in such a short amount of time. Frank and Alex were my friends and teachers and I feel very fortunate to have been given the opportunity to get to know them and work with them this summer.

## LIST OF FIGURES

Figure No.	Title	Page
1	Theoretical and experimental compositional profiles for a $\text{Hg}_{1-x}\text{Cd}_x\text{Te}$ crystal of composition $x = 0.202$ grown at $0.31 \text{ um/s}$ .	3
2	Theoretical and experimental compositional profiles of $\text{Hg}_{1-x}\text{Cd}_x\text{Se}$ ingots grown by the fast Bridgman method.	4
3	$\text{Hg}_{1-x}\text{Cd}_x\text{Se}$ phase diagram	8
4	Variations of cubic unit-cell lattice constant with $x$ in the $\text{Hg}_{1-x}\text{Cd}_x\text{Se}$ and $\text{Hg}_{1-x}\text{Cd}_x\text{Te}$ systems	10
5	Energy-band model for $\text{Hg}_{1-x}\text{Cd}_x\text{Se}$ alloys	11
6	Compositional dependence of the fundamental energy gap of $\text{Hg}_{1-x}\text{Cd}_x\text{Se}$ at $300^\circ\text{K}$	12
7	Bridgman-Stockbarger crystal growth furnace assembly	15
8	Optical micrograph of a sample taken $3.95 \text{ cm}$ from the tip of ingot A-2 ( $240\times$ )	19
9	Measured compositional profile for ingot A-2 (from precision density measurements)	22
10	Infrared transmission spectra taken on a sample $2.00 \text{ cm}$ from the tip of ingot A-2	25
11	Compositional map obtained from infrared transmission-edge mapping of a sample taken $3.95 \text{ cm}$ from the tip of ingot A-2	26
12	Compositional map obtained from infrared transmission-edge mapping of a sample taken $11.91 \text{ cm}$ from the tip of ingot A-2	27
13	Measured compositional profile for ingot A-2 (from IR transmission-edge mapping data)	30

## LIST OF TABLES

Table No.	Title	Page
1	Growth Parameters For Samples Successfully Grown To Date	18
2	Composition as Determined From Precision Density Measurements As A Function of Axial Position For Ingot A-2	21
3	Average Composition as Determined From IR Transmission Mapping As a Function of Axial Position For Ingot A-2	29

## INTRODUCTION

With an increasing emphasis on the growth of semiconducting crystals which can be used for the detection of infrared radiation and for use in the fabrication of junction devices, considerable attention has been focused on attaining a basic understanding of the mechanisms involved in the growth of homogeneous, bulk single crystals of these materials. Of particular interest is the ability to control both the longitudinal and radial compositional uniformity of directionally solidified crystals by controlling such factors as growth rate, interface shape, and temperature distributions during the growth process.

A considerable amount of work has been done to date on the HgCdTe system. There are some excellent reviews available<sup>1,2</sup> as well as a vast number of publications in the technical literature on this system. To cite just a few, which are concerned primarily with the influence of growth parameters on the solidification process of these crystals, Szofran et al.<sup>3</sup> have determined that the growth rate has a significant influence on the longitudinal compositional profile of HgCdTe crystals and that the measured radial compositional variations in these crystals also shows a strong correlation to both the growth rate as well as the temperature profile used. Bartlett, et al.<sup>4</sup> also studied the effects of growth rate on the compositional variations in HgCdTe crystals and found that again the uniformity is highly growth rate dependent. In several other works<sup>5-7</sup>, it has also been shown that the shape of the melt-crystal interface is an important factor in controlling the quality of directionally solidified HgCdTe crystals. In turn, it has been shown

that the shape of the melt-solid interface is related to the relative thermal conductivities of the solid and liquid.<sup>8,9</sup> Lehoczky and Szofran,<sup>10</sup> in a summary article, discussed the influence of all these parameters, the growth rate, the interface shape and the solid and liquid alloy conductivities, on the compositional uniformity of HgCdTe crystals. Therefore, since it has been shown that all these factors influence compositional uniformity and hence crystal quality, it is extremely important in the growth of compositionally homogeneous semiconducting crystals to have a complete understanding of both the thermophysical properties of the materials involved as well as an understanding of the influence of various growth parameters on the solidification process.

In an attempt to characterize and thus better understand the growth process of semiconducting crystals, one procedure which has been used by several investigators is to compare the experimentally measured longitudinal compositional profiles of as grown crystals to theoretical compositional profiles assuming various models. One model which appears to fit the data quite well is the one-dimensional diffusion model. In this fitting procedure, it is possible to determine an effective diffusion coefficient in the liquid. In looking at the results of this modeling by Szofran et al.<sup>3</sup> on a Bridgman grown ingot of  $\text{Hg}_{1-x}\text{Cd}_x\text{Te}$  of composition  $x=0.202$ , (Figure 1) it is seen that indeed the measured longitudinal composition profile is well modeled by the one-dimensional diffusion case. This result indicates that during the growth of HgCdTe crystals there will be a region of the crystal over which steady state solidification is proceeding and in which the average axial composition of the crystal is constant.

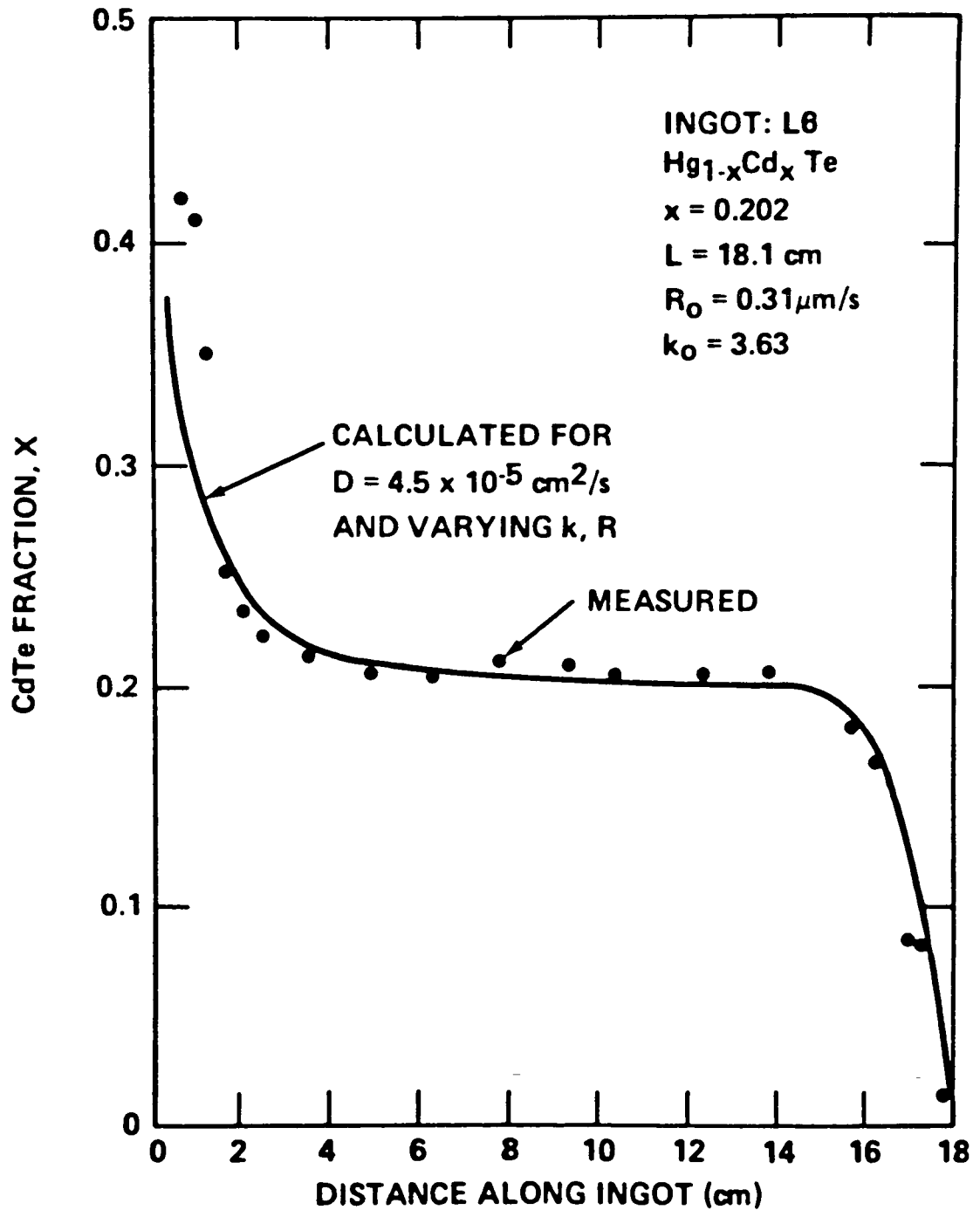


Figure 1. Theoretical and experimental profiles for a  $\text{Hg}_{1-x}\text{Cd}_x\text{Te}$  crystal of composition  $X = 0.202$  grown at  $0.31 \mu\text{m/s}$ .

In looking through the literature on semiconducting alloys, it was observed that in work done by Summers and Nelson<sup>11</sup> on a similar system, the HgCdSe system, the agreement between the measured and calculated compositional profiles, assuming a one dimensional model, was not quite as good as in the work previously quoted on HgCdTe. This lack of agreement can be seen in Figure 2. It was suspected that perhaps this disagreement, in particular the initial dip in composition followed by the continuously increasing cadmium composition throughout the normally observed steady state growth region was due to the use of a relatively fast growth rate of  $1 \mu\text{m}/\text{sec}$ .

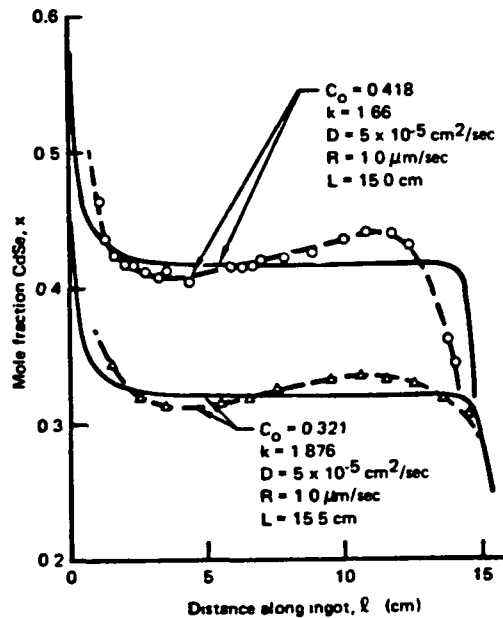


Figure 2. Theoretical and experimental compositional profiles of  $\text{Hg}_{1-x}\text{Cd}_x\text{Se}$  ingots grown by the fast Bridgman method,-----, theory;----, experiment.

In looking into this system further, it was noticed that although a considerable amount of work has been done on the HgCdTe system, a lesser amount of attention has been paid to the HgCdSe system.

Cruceanu and Niculescu<sup>12</sup>, in 1965 were the first to report in the literature the preparation of  $\text{Hg}_{1-x}\text{Cd}_x\text{Se}$  alloys. Kalb and Leute<sup>13</sup> used x-ray techniques to determine the miscibility gap limits in the HgSe-CdSe system. They determined that for  $x < 0.77$ ,  $\text{Hg}_{1-x}\text{Cd}_x\text{Se}$  alloys possess the cubic zincblende structure and that for  $x > 0.81$ , they possess the hexagonal wurtzite structure. At room temperature, the two crystallographic phases are immiscible for  $0.77 < x < 0.81$ .

Nelson, Summers, and Whitsett<sup>14</sup> determined the phase diagram for the HgSe-CdSe system using differential thermal analysis measurements. Nelson et al.<sup>15</sup> performed an experimental and theoretical study of the electron mobility in the  $\text{Hg}_{1-x}\text{Cd}_x\text{Se}$  alloy system. They grew some crystals by the Bridgman method and in their work, they discussed primarily the intrinsic and defect-scattering processes dominant in HgCdSe. A fairly comprehensive study of HgCdSe alloys was done by Whitsett, et al.<sup>16</sup> in which the preparation and characterization of HgCdSe alloys was emphasized. Several different growth methods were used in this investigation. There are a few additional studies on HgSe and HgCdSe, however, this brief review accounts for the majority of the published work on the growth of HgCdSe crystals.

There are several reasons for the rather limited work on this system in comparison to the HgCdTe system. One primary reason is that HgCdSe is an n-type semiconductor as grown and remains so under all types of subsequent treatment. This, coupled with the fact that the carrier

concentration is quite high ( $10^{18}$ ) in the as grown state, poses several problems in the utilization of HgCdSe for many applications. In contrast, HgCdTe is p-type as grown and can be made n-type by annealing in a mercury vapor. This capability adds greater flexibility in the area of device production.

Also, HgCdSe appears to be quite unstable electrically, thus making its commercial utilization at this time unattractive. However, the lattice characteristics of HgCdSe are quite favorable for growing strain free crystals and if a better understanding of the system can be obtained, it may prove to be a feasible system for further investigation and development.

Therefore, because of the limited published results on the HgCdSe system, coupled with the interesting results of Summers and Nelson,<sup>11</sup> and the apparent potential usefulness of HgCdSe as a semiconducting material provided certain instabilities can be overcome, it was decided to further investigate this system.

#### OBJECTIVE

The objective of this work was to gain a better understanding of the influence of growth parameters on the compositional uniformity of Bridgman grown HgCdSe crystals. In particular, it was decided to determine the influence of growth rate on both the longitudinal and radial compositional uniformity of HgCdSe crystals of fixed composition. These crystals were directionally solidified in a Bridgman-type crystal growth furnace and their compositional profiles, both axially and

radially, were determined using precision density measurements and infrared transmission edge mapping.

An ultimate objective of this project will be to compare the measured longitudinal profiles with the theoretical model for a one-dimensional diffusion case and to determine an effective diffusion coefficient. Also, it is desired to utilize the radial compositional variations in conjunction with the particular growth parameters to infer the thermophysical properties of the material.

### HgSe-CdSe SYSTEM

HgSe crystallizes in the zincblende structure and CdSe crystallizes in the wurtzite structure. These two compounds combine to form what is referred to as a pseudobinary system which is shown in Figure 3. As noted on this diagram, and determined by Kalb and Leute,<sup>13</sup> this system contains a small miscibility gap. The existence of this peritectic reaction at 947° does not appear to disturb significantly the solidus and liquidus curves which vary smoothly between HgSe and CdSe.

HgSe – CdSe PSEUDOBIINARY ALLOY SYSTEM

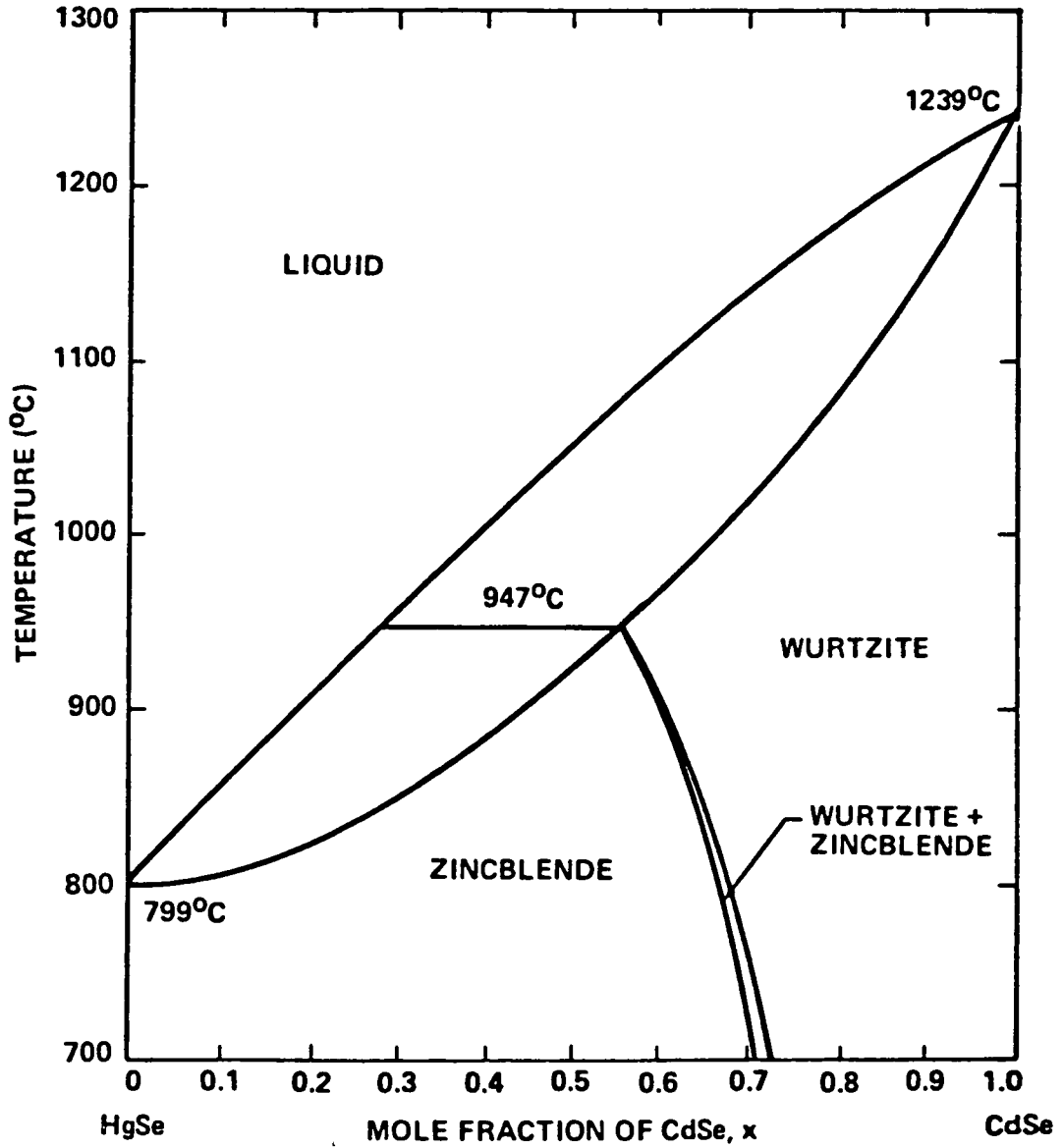


Figure 3.  $Hg_{1-x}Cd_xSe$  phase diagram

Pseudobinary alloys of HgSe and CdSe are commonly represented by the formula  $\text{Hg}_{1-x}\text{Cd}_x\text{Se}$  where  $x$  is the mole fraction of CdSe. With increasing values of  $x$ , it is seen in Figure 4 that the variation in lattice constant is quite small, with the variation being smaller than that for the HgCdTe system. This would be advantageous in the growth of HgCdSe crystals because slight variations in composition would not result in significant strains being introduced in the crystals due to lattice constant changes.

Mercury selenide is classified as a perfect semimetal or symmetry-induced zero-gap semiconductor. On the other hand, cadmium selenide is a wide gap semiconductor with a fundamental direct band gap of 1.8eV. When HgSe and CdSe combine to form  $\text{Hg}_{1-x}\text{Cd}_x\text{Se}$ , the energy gap increases continuously from a small negative value for HgSe to a larger positive value as a function of  $x$ . This transition is represented schematically in Figure 5. Thus, it is possible by varying the alloy composition to tailor the band gap of HgCdSe crystals and hence the wavelength at which they become transparent to infrared radiation. Figure 6 from Whitsett, et al.<sup>16</sup> shows this relationship between the band gap and  $x$  at 300°K.

However, the electrical properties of HgCdSe are quite unstable thus making its use commercially unattractive at this time. Nevertheless, as mentioned earlier, the lattice characteristics are quite desirable as far as growing strain free crystals and if the system can be better understood and controlled, it may prove to be a feasible system for further investigation and development.

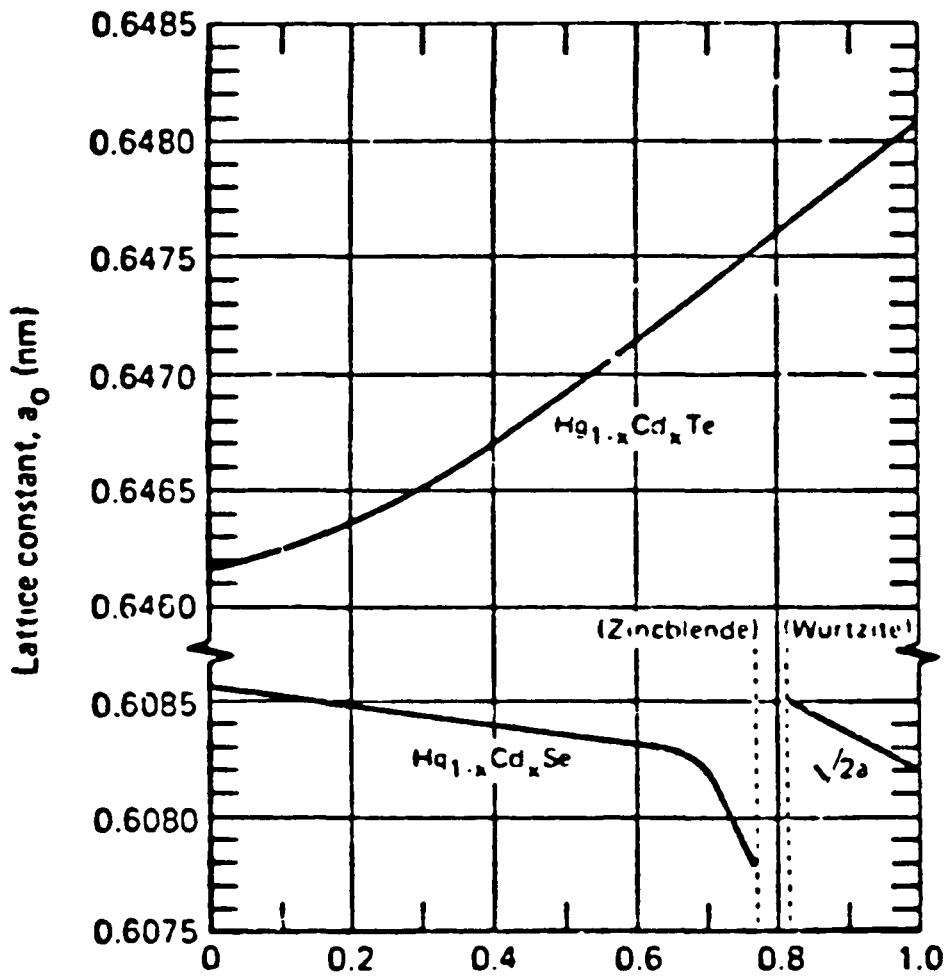


Figure 4. Variations of cubic unit-cell lattice constant with  $x$  in the  $Hg_{1-x}Cd_xTe$  and  $Hg_{1-x}Cd_xSe$  systems

$\text{Hg}_{1-x}\text{Cd}_x\text{Se}$  BAND STRUCTURE

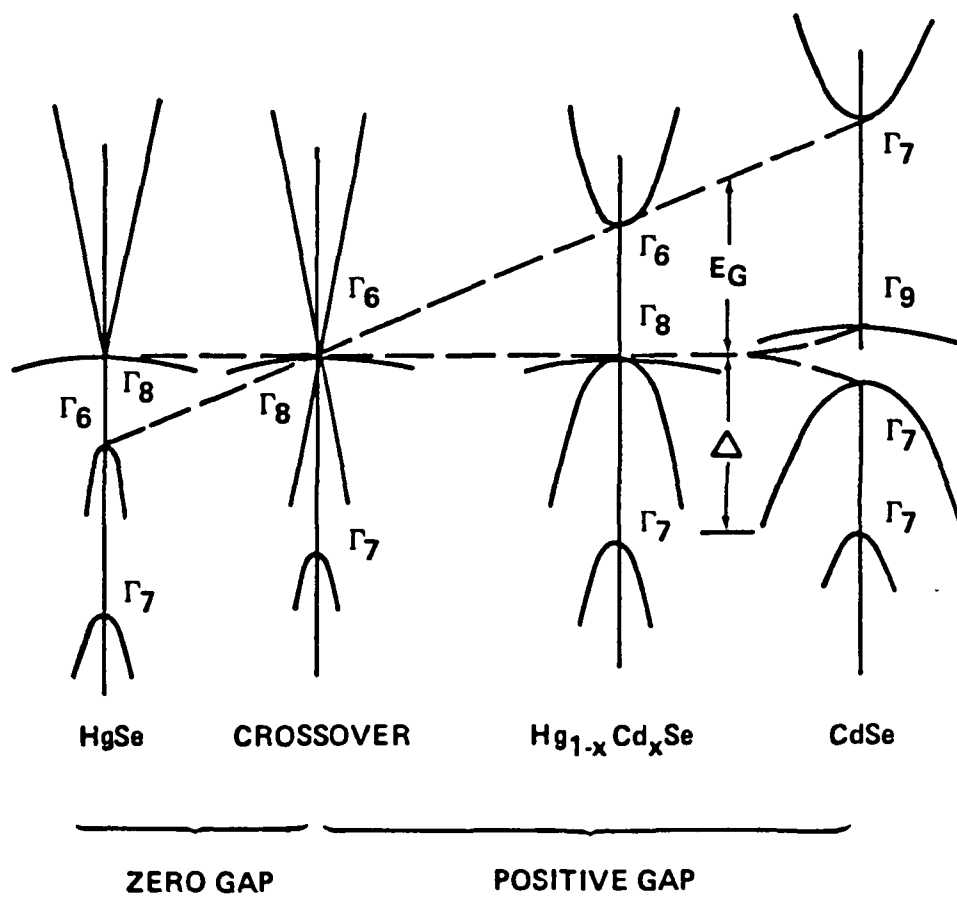


Figure 5. Energy-band model for  $\text{Hg}_{1-x}\text{Cd}_x\text{Se}$  alloys

BAND GAP ENERGY AS A FUNCTION OF COMPOSITION

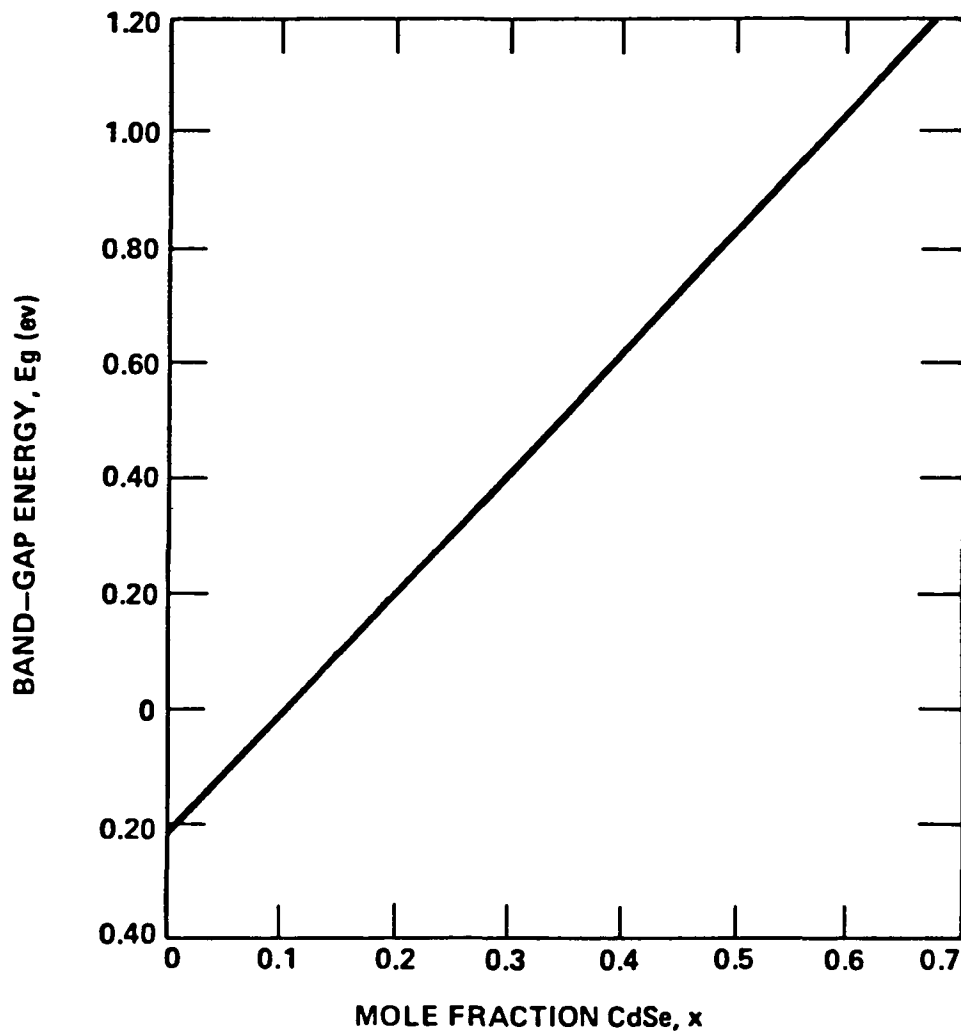


Figure 6. Compositional dependence of the fundamental energy gap of  $Hg_{1-x}Cd_xSe$  at 300°K

### EXPERIMENTAL PROCEDURE

All alloys used in this investigation were prepared by reacting 5-9's pure selenium(Se) 6-9's pure cadmium(Cd) and 7-9's pure mercury(Hg) in sealed, evacuated quartz ampoules of 5mm I.D, 10mm O.D., and 40 cm in length. The quartz ampoules were tapered to a point on one end to facilitate single crystal growth during subsequent directional solidification. The ampoules were first cleaned thoroughly with methanol and water and annealed at 1140°C for approximately three hours to relieve any strains induced during previous glass working processes.

Stoichiometric amounts of Hg, Cd, and Se were precisely weighed out for an alloy composition of  $x=0.200$ . The Cd and Se were inserted into the tube and the Hg was weighed into a glass container for subsequent insertion into the ampoule. The ampoule and the glass container holding the mercury were assembled and attached to a vacuum system through an O-ring fitting. The system was evacuated to a pressure of approximately 10 millitorr. The mercury was then inserted into the ampoule and the ampoule was sealed off.

The ampoule containing the Hg, Cd, and Se was then wrapped in high temperature wool and placed in a quartz lined inconel tube inside a rocking furnace. Care was taken to ensure that the ampoule was in the center of the tube furnace. The furnace was heated up slowly, particularly through the 700°C range. After the solidus temperature was reached, the furnace was rocked in an attempt to homogenize the alloy. After reaching the maximum temperature, which ranged from 80°C to 160°C above the liquidus temperature, the furnace was rocked for an additional

fifteen hours. At the end of this time, the furnace was oriented in a slightly inclined position from horizontal and the tip of the ampoule was lowered out the bottom of the furnace. This was done to initiate solidification at the ampoule tip.

After solidification, the ampoule was placed in a Bridgman-type directional solidification furnace. The alloy was remelted, and then directionally solidified at a particular growth rate and under specific thermal conditions.

A diagram of the furnace is shown in Figure 7. In this configuration, the quartz ampoule is placed on a quartz pedestal, and at the beginning of the growth process is positioned in the upper furnace. The ampoule remains stationary throughout the process and the furnace translates upwards. The furnace assembly consists of two resistively heated tubular furnaces with an upper hot zone and a lower cold zone. The two heat zones are well defined and isothermal due to the use of a sodium heat pipe in the upper zone and a potassium heat pipe in the lower zone. The two heat pipes are separated by a thermal barrier, the thickness of which is variable depending on the desired temperature profile for the particular growth process. Barrier thicknesses used in this study were 2.4cm and 0.64cm. The circular opening in the barrier was 1.19cm.

Before each crystal growth experiment, a temperature profile of the furnace was recorded to establish the thermal conditions present in the furnace. The profile is dependent on the particular combination of upper and lower zone temperatures as well as the barrier thickness. The particular profile which exists in the furnace determines the relative position of the solid-liquid interface with respect to the barrier.

ORIGINAL PAGE IS  
OF POOR QUALITY

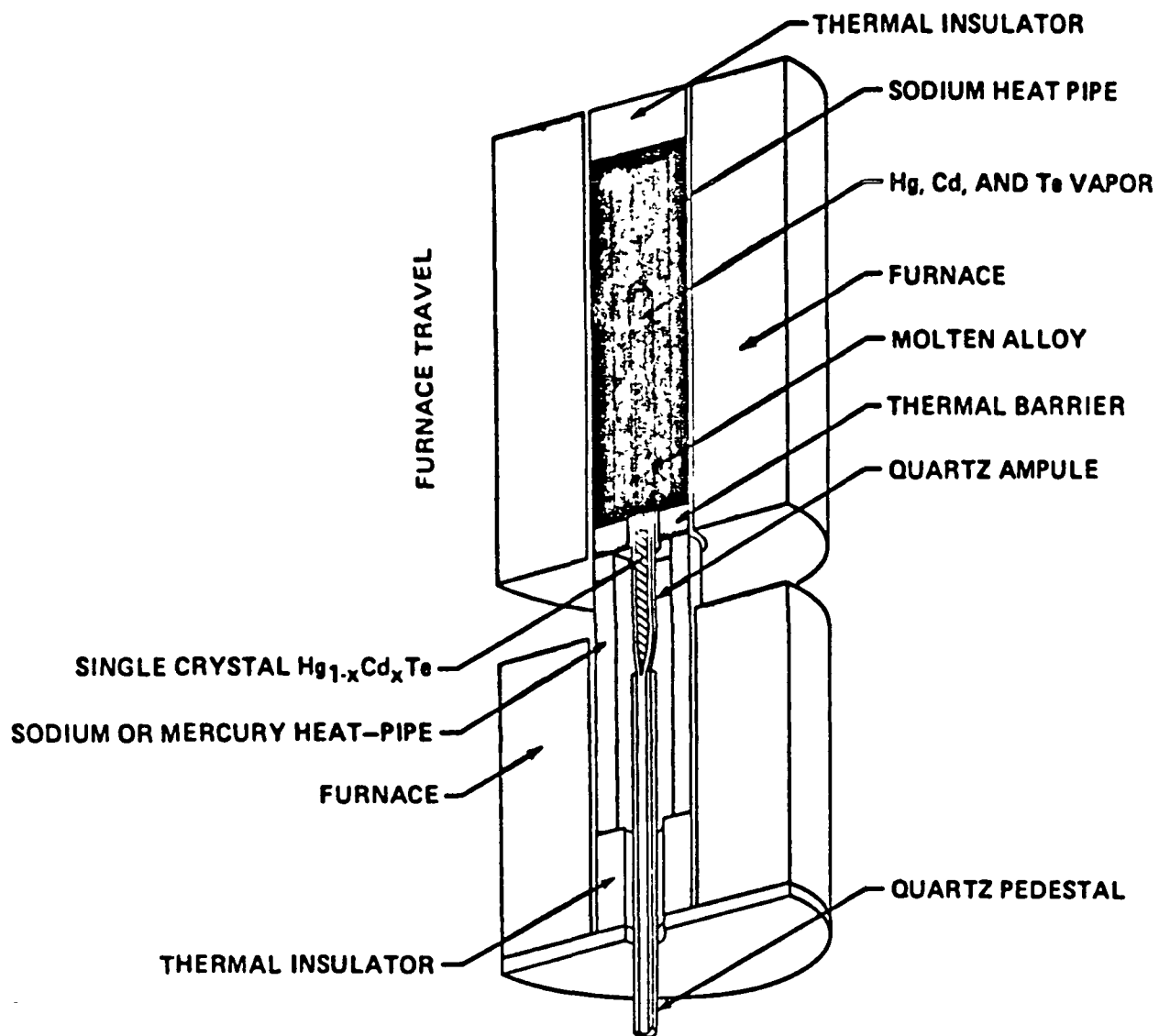


Figure 7. Bridgman-Stockbarger crystal-growth furnace assembly

The proper positioning of this interface is quite important in that it may directly affect the shape of the interface and hence the radial compositional uniformity.

The thermal gradient at the interface also is an important consideration in the growth of semiconducting crystals in that it must be steep enough to prevent constitutional supercooling. Of primary importance is the gradient at the solidus temperature, corresponding to the steady state growth interface. However, care must also be taken to ensure that the thermal gradient is steep enough at the liquidus temperature where initial solidification begins. From a knowledge of the initial segregation coefficient,  $k$ , and the thermal gradient  $G$  obtained from a temperature profile, the maximum permissible growth rate which should avoid constitutional supercooling was determined using the following relationship:

$$G/R = \frac{mC_0(k-1)}{Dk} \text{ where}$$

$m$  = the slope of the liquidus curve at the composition of interest

$C_0$  = mole fraction CdSe

$D$  = the diffusion coefficient

$R$  = growth rate

$k$  = segregation coefficient

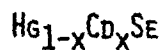
## RESULTS AND DISCUSSION

At the time of this writing, three crystals, designated A-2, A-4, and A-5 have been successfully grown. The growth parameters for each are listed in Table 1. Ingot A-2 has been almost fully characterized at this time and the results of the analysis will be the primary focus of this report. As seen in Table 1, ingot A-4 was grown at a faster growth rate than ingot A-2, but with a thinner barrier in an attempt to increase the thermal gradient present at the beginning of solidification to prevent constitutional supercooling. Ingot A-5 was grown with a relatively steep thermal gradient, this time with a thick barrier in an attempt to ensure that the steady state position of the growth interface was well within the barrier. The intent was to look at the shape of the solid-liquid interface resulting from these growth conditions in an attempt to obtain some information about the thermal properties of the liquid relative to the solid.

Three primary characterization techniques were utilized in this study. Optical microscopy, precision density measurements, and infrared transmission-edge mapping were used to obtain information about the microstructure and the compositional uniformity of the alloys. These results will be presented and discussed in the following sections.

TABLE 1  
GROWTH PARAMETERS FOR  
SAMPLES SUCCESSFULLY GROWN TO DATE

INGOT A-2



$$x = 0.2$$

$$L = 16.7 \text{ cm}$$

$$\text{GROWTH RATE (R)} = 0.3 \text{ } \mu\text{M/s}$$

$$\text{THERMAL GRADIENT (G)} = 97^\circ \text{ C/cm}$$

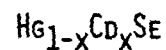
$$k = 2.25$$

$$\text{BARRIER: } 2.4 \text{ cm}$$

$$T_U = 960^\circ\text{C}$$

$$T_L = 486^\circ\text{C}$$

INGOT A-4



$$x = 0.2$$

$$L = 16.8 \text{ cm}$$

$$R = 0.4 \text{ } \mu\text{M/s}$$

$$G = 187^\circ\text{C/cm}$$

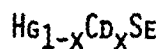
$$\text{BARRIER: } 0.64 \text{ cm}$$

$$\text{ANNEALED AT } 250^\circ\text{C FOR 2 DAYS}$$

$$T_U = 1015^\circ\text{C}$$

$$T_L = 417^\circ\text{C}$$

INGOT A-5



$$x = 0.2$$

$$L = 16.4 \text{ cm}$$

$$R = 0.3 \text{ } \mu\text{M/s}$$

$$G = 90^\circ\text{C/cm}$$

$$\text{BARRIER: } 2.4 \text{ cm}$$

$$T_U = 1000^\circ\text{C}$$

$$T_L = 670^\circ\text{C}$$

## MICROSCOPY

All samples were ground and polished using standard metallographic procedures down to a polish on 0.25um diamond. They were etched for 15 seconds in Straughn's reagent at 60°C and then rinsed in a dilute solution of bromine in methanol, followed by rinses in methanol.

The microstructure of a sample taken at 3.95cm from the tip of ingot A-2 is shown in Figure 8. As can be seen, a fine cell structure is evident. This indicates an interface instability and the possibility that the initial thermal gradient was not steep enough and as a result, a slight amount of constitutional supercooling occurred.

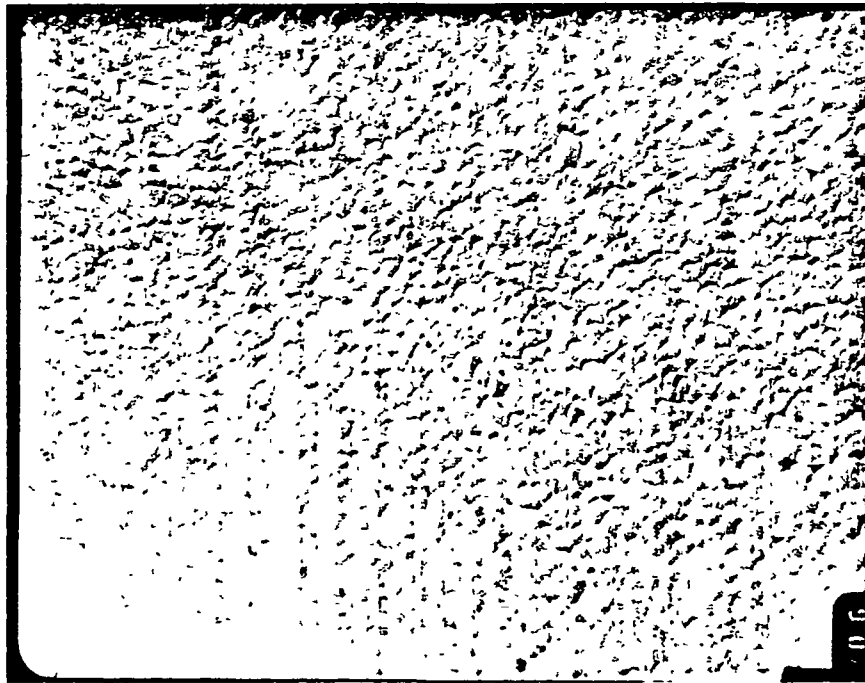


Figure 8. Optical micrograph of a sample taken 3.95cm from the tip of ingot A-2 (240x)

However, in analyzing a slice taken at 14.91cm from the tip of A-2, no apparent microstructure was observed. This seemed to indicate that once steady state growth was achieved, constitutional supercooling was eliminated. This would be expected, since the thermal gradient at the solid-liquid steady state interface was steeper than that at the liquidus. No grain boundaries were observed in the slice examined, however, x-ray analysis is needed to confirm the presence of a single crystal.

#### PRECISION DENSITY MEASUREMENTS

Iwanowski<sup>17</sup>, in 1975, showed that the mass density of  $Hg_{1-x}Cd_xSe$  decreases linearly with increasing x value, through both the zincblende and wurtzite structures. Therefore, precision density measurements can be used to accurately determine alloy composition. Precision density measurements were made in accordance with the procedure described by Bowman and Schooner<sup>18</sup>. Table 2 summarizes the results of the density measurements for slices taken at various distances along the length of the ingot A-2. Figure 9 graphically shows the relationship between the measured axial density and the distance from the ampoule tip. As can be seen, the overall trend appears to be well modeled by the one-dimensional diffusion case, that is, an initial transient is observed, followed by a steady state growth region, ending up with a final transient.

At a distance of 6.41cm from the ampoule tip, it is seen that the average composition of the solid increased. This rise in composition is well correlated with an actual stopping of the furnace translation due to a motor failure.

TABLE 2

COMPOSITION AS DETERMINED FROM PRECISION DENSITY MEASUREMENTS AS A FUNCTION OF AXIAL POSITION FOR INGOT A-2

<u>DISTANCE FROM TIP</u> (CM)	<u>COMPOSITION</u>
1.00	0.289
1.55	0.247
2.00	0.223
3.05	0.204
3.55	0.213
3.95	0.202
5.55	0.213
6.41	0.245
8.52	0.206
9.25	0.204
9.95	0.182
10.98	0.182
11.91	0.204
12.91	0.182
13.71	0.175
14.91	0.165
15.15	0.155
15.35	0.138
15.50	0.103
15.75	0.054
15.90	0.022

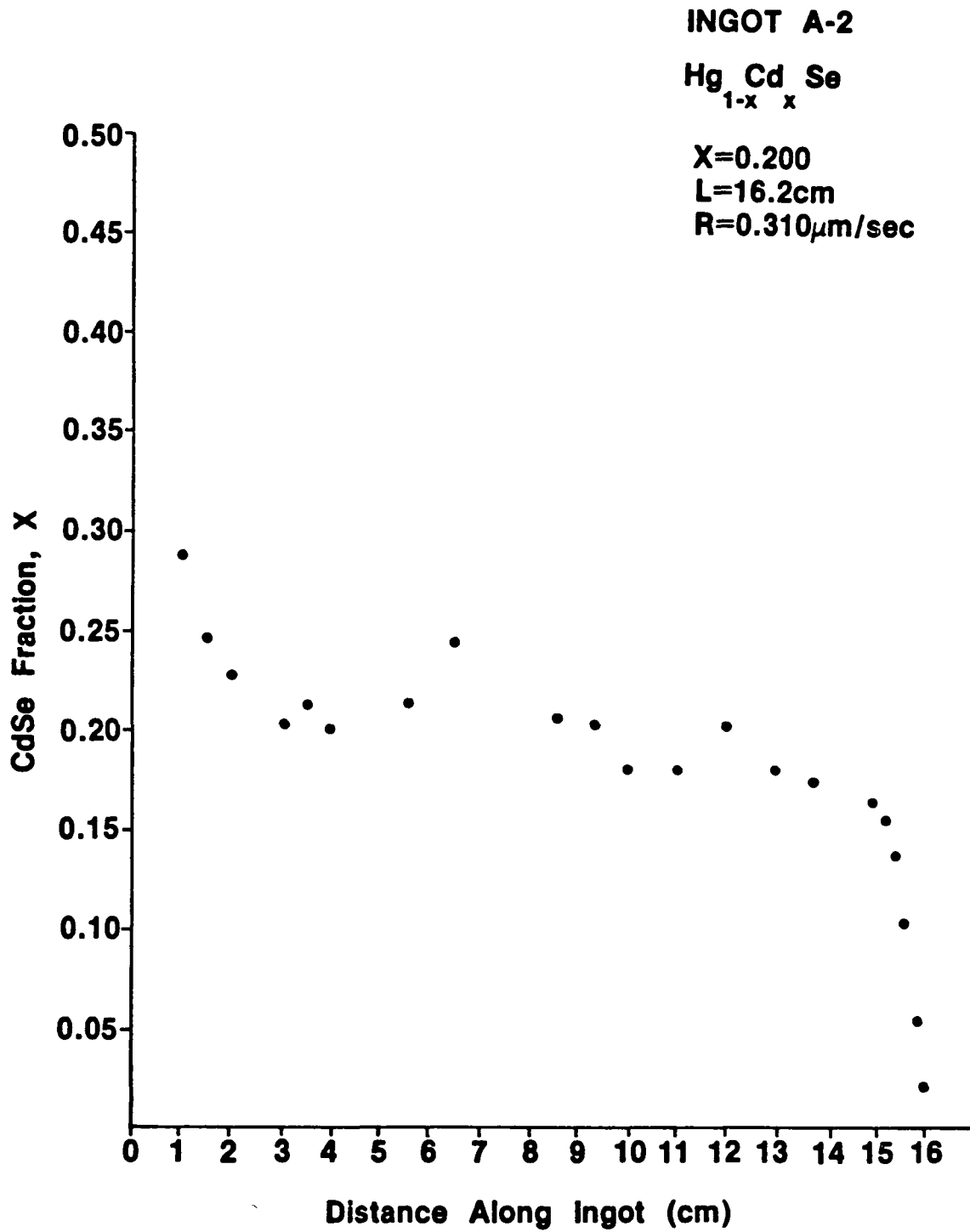


Figure 9. Measured compositional profile for ingot A-2 (From precision density measurements)

It is apparent that the composition along the ingot was approaching a steady state value when the translation stopped. However, as the alloy remained stationary with respect to the furnace, the system began to return to an equilibrium state, and thus, upon resuming translation, another transient is observed, followed by a subsequent movement into a steady state region.

Further analysis is currently underway on material sectioned from this interrupted region and is showing some interesting results. The results have prompted additional experiments which could provide some very exciting insights into the interface stability and diffusion in this system.

#### IR TRANSMISSION MAPPING

Infrared transmission mapping is a technique which can be used to determine the radial compositional uniformity of thin slices taken along the length of a crystal. It also is possible to utilize this technique to get an average  $x$  value for the slice. However, the outermost edges of the sample, which in this experiment are lowest in  $x$  value, are not included in the IR analysis. As a result, the average  $x$  value obtained by this method will be slightly higher than the  $x$  value obtained by precision density measurements, however density trends should be fairly similar.

Slices of approximately 1mm thickness were cut along the length of ingot A-2, ground to about 0.75mm thickness and etched with a methanol-5% bromine solution. All transmission measurements were made at room temperature at regularly spaced intervals on each slice. To improve spatial resolution, an aperture 100  $\mu\text{m}$  in diameter was used.

Typical results for a spectra obtained from a slice 2.00cm from the tip of ingot A-2 is shown in Figure 10. Pairs of curves correspond to symmetrical points on the sample, with the outermost curve representing the center of the slice. As can be seen in this plot of transmission vs wavenumber, a wavenumber corresponding to the cut-on where the crystal goes from being transparent to opaque can be obtained, and this wavenumber which corresponds to a particular gap energy can be used to obtain an x value, since, as discussed earlier, the energy band gap of a  $\text{Hg}_{1-x}\text{Cd}_x\text{Se}$  crystal can be directly related to the alloy composition. This relationship is also temperature dependent and can best be expressed by the following equation:<sup>11</sup>

$$E_g = -0.209(1-7.172x-2.17x^2) \\ +7.37 \times 10^{-4}(1-1.277x-0.151x^2)T \\ +2.00 \times 10^{-9}(1+23.45x-599.4x^2)T^2$$

Typical results of radial compositional profiles are shown in Figures 11 and 12. As can be seen here, the ingot, as grown, is cadmium rich in the center and cadmium deficient on the edges. This finding was quite surprising since it is directly opposite to that commonly observed in the  $\text{Hg}_{1-x}\text{Cd}_x\text{Te}$  system. Such variations suggest a convex interface for the entire growth length. Such an interface shape can have definite implications as to the thermophysical properties of this system and this area is currently being investigated further as a continuation of this project.

### A-2 2.00 with 100 um Aperture

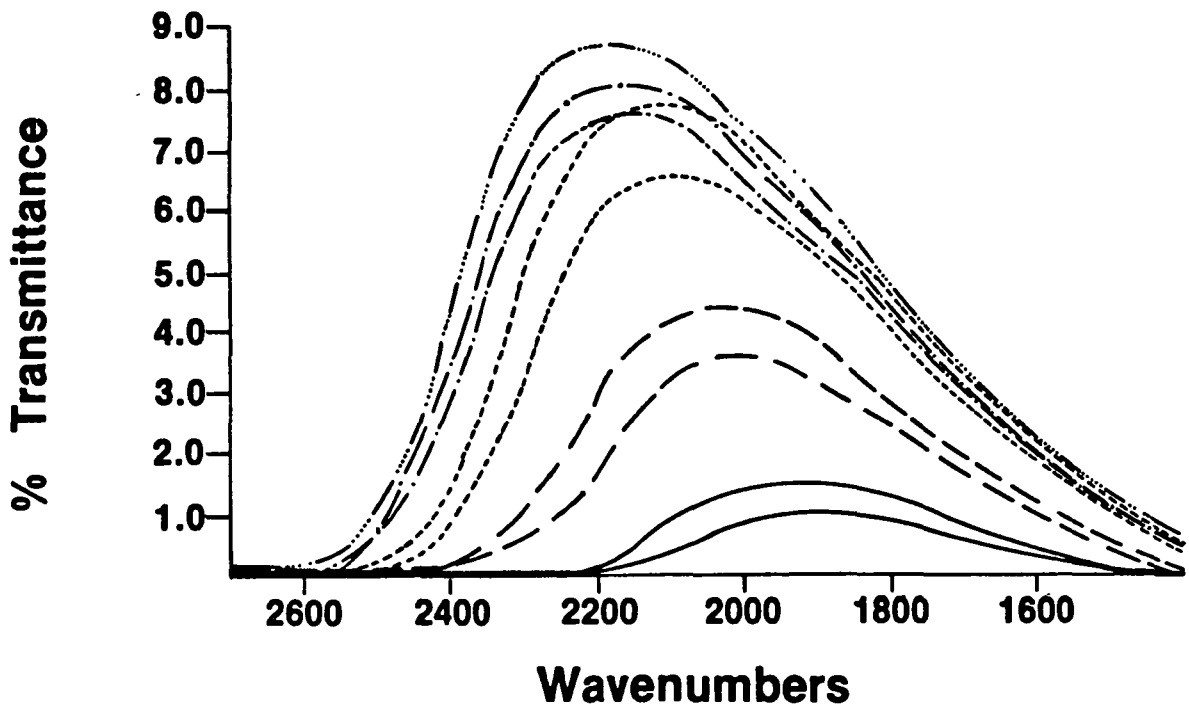


Figure 10. Infrared transmission spectra taken on a sample 2.00cm from the tip of ingot A-2

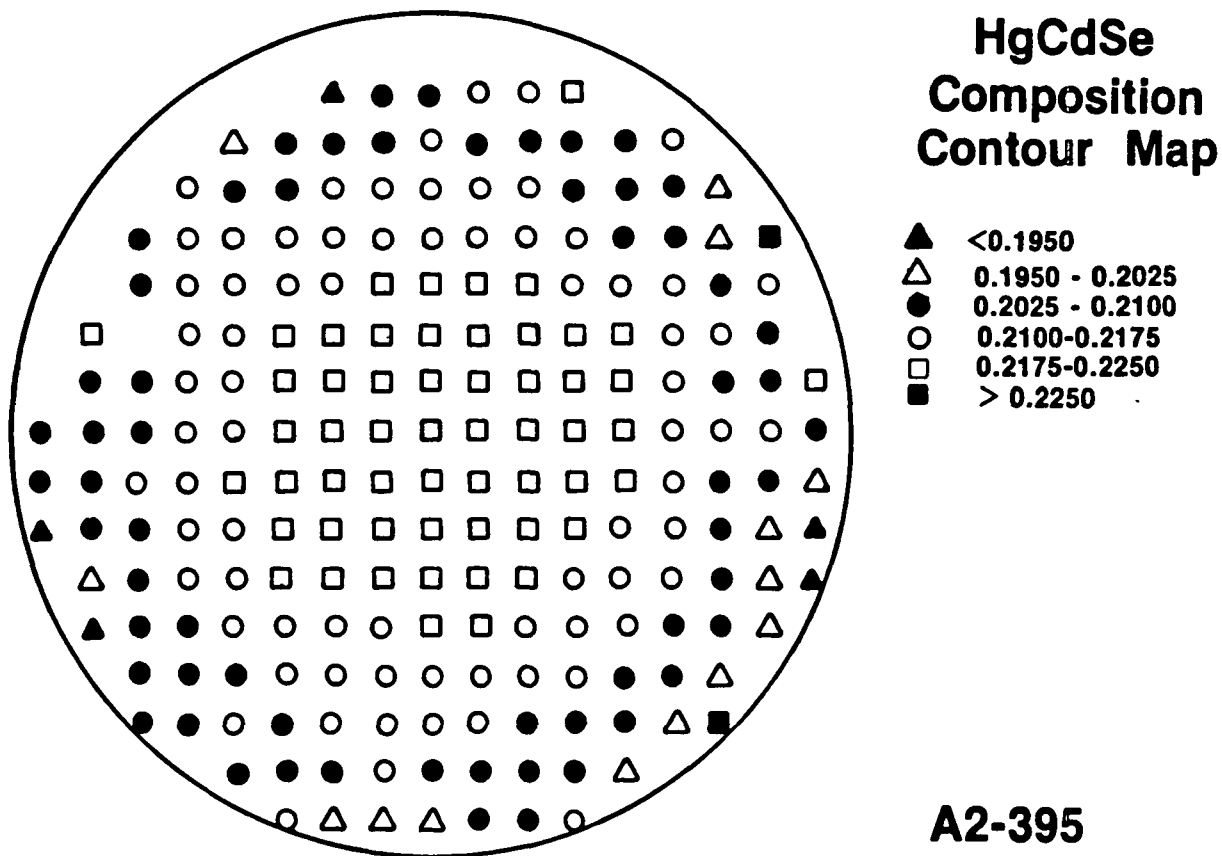


Figure 11. Compositional map obtained from infrared transmission-edge mapping of a sample taken 3.95cm from the tip of ingot A-2

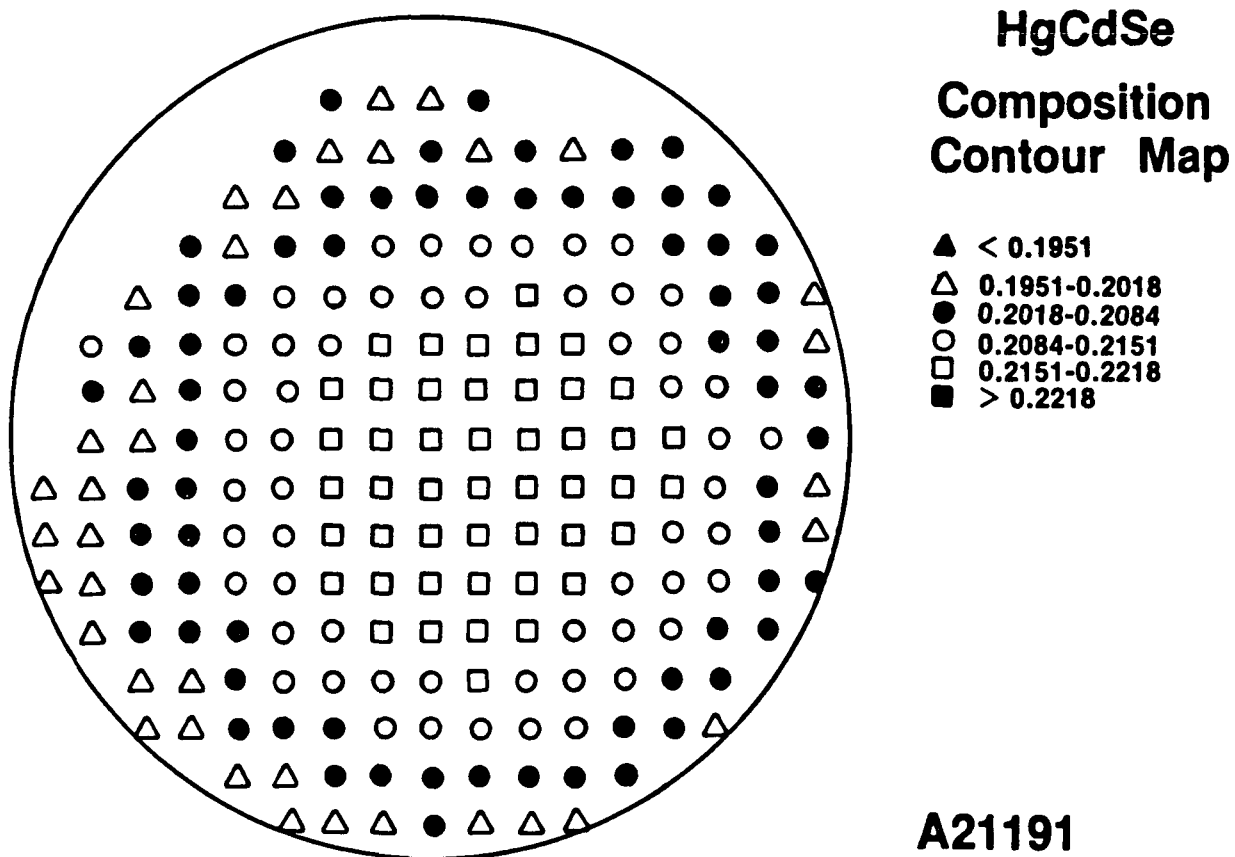


Figure 12. Compositional map obtained from infrared transmission-edge mapping of a sample taken 11.91cm from the tip of ingot A-2

Table 3 is a tabulation of the average  $x$  value obtained by IR mapping for each slice taken from ingot A-2. A plot of this average composition ( $x$ ) of each radial slice as a function of distance from the tip is shown in Figure 13. As can be seen from this figure, the axial compositional profile appears at a first approximation to be well modeled by the one-dimensional diffusion model. The length of the steady state region of growth also indicates that the diffusion coefficient,  $D$ , in this system may in fact be lower than that in the HgCdTe system. This is also a very interesting finding, since it was initially assumed that they would be approximately the same.

TABLE 3

AVERAGE COMPOSITION AS DETERMINED FROM IR  
TRANSMISSION MAPPING AS A FUNCTION OF AXIAL  
POSITION FOR INGOT A-2

<u>DISTANCE FROM TIP</u>	<u>COMPOSITION</u>
1.55	.235
2.00	.218
3.05	.211
3.55	.209
3.95	.212
4.51	.207
5.55	.203
6.41	.236
8.52	.199
9.25	.204
9.95	.206
10.98	.206
11.91	.209
12.91	.206
13.71	.202
14.91	.191

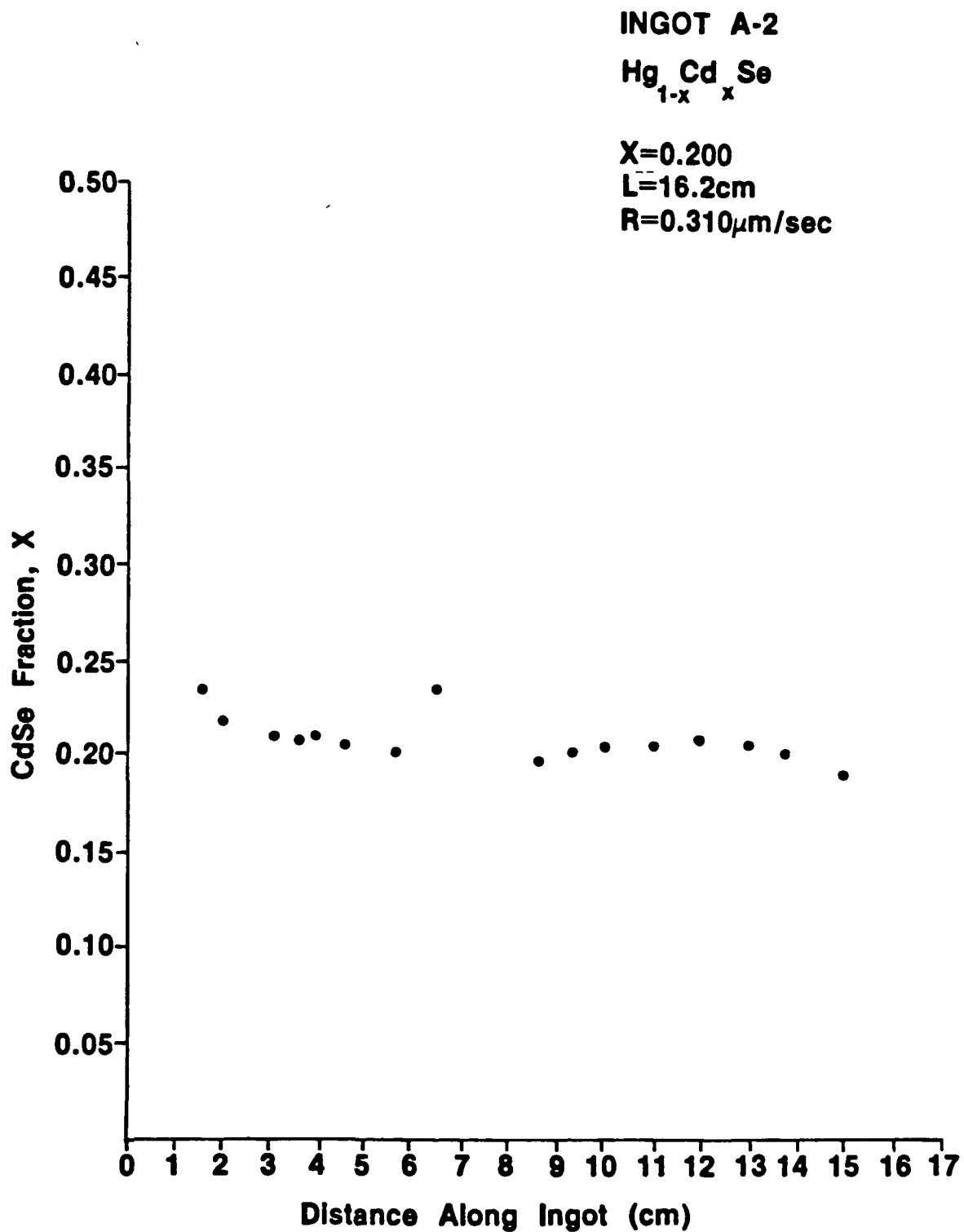


Figure 13. Measured compositional profile for ingot A-2 (from IR transmission edge-mapping data)

## TENTATIVE CONCLUSION

At this time it is difficult to make definite conclusions. However, based upon the preliminary results of this investigation, the following tentative conclusions can be made:

1. The results of the longitudinal composition profile on a Bridgman grown crystal of  $\text{Hg}_{1-x}\text{Cd}_x\text{Se}$  of composition  $x = 0.2$ , grown at  $0.3\mu\text{m}/\text{sec}$ , (ingot A-2) appears to be well modeled by the one-dimensional diffusion model. This suggests that the results of Summers and Nelson<sup>11</sup> were influenced by constitutional super cooling.
2. The radial composition profile of ingot A-2 consists of a cadmium rich center and hence implies a convex growth interface. This is opposite to that of the  $\text{Hg}_{1-x}\text{Cd}_x\text{Te}$  system and this in turn implies differences in the thermophysical properties of the two systems.
3. Due to the length of the steady state growth region in the axial composition profile, the diffusion coefficient in the liquid in the  $\text{HgCdSe}$  system appears to be less than in the  $\text{HgCdTe}$  system.

Further experimentation is currently underway and planned. Evaluation of the results will be necessary to confirm or modify the above conclusions. Also, crystal growth experiments are planned which will be used to evaluate the influence of the growth rate on compositional uniformity.

As mentioned previously, ingot A-4, grown at 0.4um/sec, is currently being evaluated, as well as ingot A-5, grown at 0.3um/sec utilizing different thermal conditions in the growth furnace. These results will provide a better understanding between thermal conditions and interface shape.

## REFERENCES

1. R. K. Willardson, A. C. Beer, Ed., Semiconductors and Semimetals, Vol 18., (Academic Press, New York, 1981).
2. J. L. Schmit, J. of Crystal Growth 65 (1983) 249
3. F. R. Szofran, D. Chandra, J. C. Wang, E. K. Cothran, and S. L. Lehoczky, J. of Crystal Growth 70 (1984) 343
4. B. E. Bartlett, P. Capper, J. F. Harris, and M.J. T. Quelch, J. of Crystal Growth, 46 (1979) 623.
5. C. L. Jones, P. Capper, J. J. Gosney, and I. Kenworthy, J. of Crystal Growth, 69 (1984) 281.
6. F. R. Szofran and S. L. Lehoczky, J. of Crystal Growth, 70 (1984) 349.
7. C. E. Chang, and W. R. Wilcox, J. of Crystal Growth, 21, (1974) 135
8. C. E. Huang, D. Elwell, and R. S. Feigelson, J. Crysstal Growth 64 (1983) 441
9. R. J. Naumann and S. L. Lehoczky, J. Crystal Growth 61 (1983) 707
10. S. L. Lehoczky and F. R. Szofran, in: Materials Processing in the Reduced Gravity Environment of Space, Vol. 9, Ed. G. E. Rindone (North-Holland, New York, 1982) p. 409
11. C. R. Whitsett, J. G. Broerman, and C. J. Summers, in: Semiconductors and Semimetals, Vol. 16, Ed. R. K. Willardson and A. C. Beer, (Academic Press, New York, 1981)
12. E. Cruceana and D. Niculescu, Compt. Rend. 261 (1965) 931
13. A. Kalb and V. Leute, Phys. Stat. Sol. (a), 5 (1971) K199

14. D. A. Nelson, C. J. Summers, and C. R. Whitsett, J. Electron. Mater. 6 (1977) 507
15. D. A. Nelson, J. G. Broerman, C. J. Summers, and C. R. Whitsett, Physical Review B, 4 Vol 18, (1987) 1658.
16. C. R. Whitsett, J. G. Broerman, D. A. Nelson, and C. J. Summers, Final Report MDRL Contract N00014-74-C-0318 (ONRC) (1976)
17. R. J. Iwanowski, Acta Physica Polonica, Vol. A 47, 5, (1975)
18. H. A. Bowman and R. M. Schooner, J. Res. Natl. Bur Std., 71C(1967)179